PAPER

NJC
www.rsc.org/njc

Synthesis, characterization and magnetic properties of disk-shaped particles of a cobalt alkoxide: $Co^{II}(C_2H_4O_2)$

Nassira Chakroune,[a] Guillaume Viau,*[a] Souad Ammar,[a] Noureddine Jouini,[b] Patrick Gredin,[c] Marie Josèphe Vaulay[a] and Fernand Fiévet[a]

[a] *ITODYS (CNRS UMR 7086), Université Paris 7-Denis Diderot, case 7090, 2 place Jussieu, F-75251 Paris cedex 05, France. E-mail: viau@ccr.jussieu.fr*
[b] *Laboratoire des Propriétés Mécaniques et Thermodynamiques des Matériaux (CNRS UPR 9001), Institut Galilée, 99 avenue J. B. Clément, 93430 Villetaneuse, France*
[c] *Laboratoire de Cristallochimie du Solide, Université Paris 6-Pierre et Marie Curie, 4 place Jussieu, F-75251 Paris cedex 05, France*

Received (in Montpellier, France) 20th July 2004, Accepted 4th October 2004
First published as an Advance Article on the web 10th January 2005

A cobalt alkoxide, $Co(OCH_2CH_2O)$, has been prepared from the reaction of cobalt acetate with ethanediol. This compound crystallizes as disk-shaped particles with diameter and thickness in the 0.4–1 μm and 100–250 nm ranges, respectively. Structural characterization (X-ray and electron diffraction) shows a layered arrangement with a brucite-like structure presenting a turbostratic disorder. The interlayer spacing and the Co···Co distance within the layer are $c = 8.27$ Å and $a = 3.09$ Å, respectively. UV-visible spectroscopy studies established that the Co(II) ions are located on octahedral sites. IR spectroscopy showed that the ethylene glycolate anions $(OCH_2CH_2O)^{2-}$ chelate the Co(II) cations. The magnetic properties of the compound were measured in the range of 2–300 K. Below 20 K, the compound exhibits 3D ferromagnetic order and the hysteresis loop shows a very high remanence-to-saturation ratio typical of a uniaxial magnetocrystalline anisotropy.

1. Introduction

Several reports in the past two decades have shown that liquid polyols are suitable media for the elaboration of a great variety of inorganic compounds: monodisperse metal and oxide particles in the nanometer and micrometer size range, and layered hydroxy salts (LHS). The competition between hydrolysis and reduction is controlled by two factors: the amount of water and the working temperature. Absence of water favors reduction and, thus, the formation of metals. Conversely, the presence of water inhibits reduction, favors hydrolysis, and leads to the formation of oxides and hydroxy salts.[1] Noble metals,[2] 3d transition metals, such as Co,[3] Ni [4] and Cu,[5] and CoNi [6] and FePt [7] magnetic alloys were obtained by reduction of the corresponding precursor salts in α-diols. The polyol acts as a solvent for the metal salts, and as a reducing agent and growth medium for the metal particles.[8] By increasing the amount of water over that used for metals, nanoparticles of oxides with a spinelle-like structure were prepared in polyols.[9] Fine particles of zinc oxide,[10] metastable $Zn_xCo_{1-x}O$ solid solutions[11] and rare earth oxides[12] were also prepared by hydrolysis in liquid polyols. Furthermore, liquid polyols are an interesting media for the synthesis of Co, Ni and Zn LHS hydroxyacetates.[13]

The formation of these compounds in liquid polyols is preceded by the dissolution of the precursor salt, generally an acetate or hydroxide. This implies that reduction and hydrolysis should occur on complex species formed *in situ* in the polyol medium. The characterization of such species should lead to a better understanding of the formation mechanism of inorganic compounds in polyols. In the case of zinc, the formation of zinc oxide or LHS is preceded by the formation of an *in situ* alkoxyacetate complex. Crystals were obtained in ethanediol (ethylene glycol) and diethylene glycol, and the structural resolutions clearly showed that polyol and acetate anions complex the metal cations to form alkoxide species.[14] The hydrolysis of this species leads, as in the sol-gel method, to the hydroxy salt or oxide, depending on the amount of water and the working temperature. In the case of nickel and cobalt, metal and oxide particles are generally obtained after precipitation and re-dissolution of a solid intermediate phase.[8] Thus, in the case of nickel, two main intermediate phases have been identified. The nickel alkoxide $Ni(OCH_2CH_2O)$ was obtained by heating nickel hydroxide in ethanediol and distilling off the water formed.[15] A distorted brucite-like structure was inferred from powder X-ray diffraction.[15] If an acetate ion is present along with water, the LHS hydroxyacetate salt is obtained.

In the case of cobalt, several alkoxides have been recently prepared by Larcher *et al.*[16] in different α-diols. The alkoxide powders were used as precursors of oxide powders through thermal decomposition. This approach allowed the synthesis of oxide particles with controlled morphology and texture.[16] To the best of our knowledge the cobalt(II) alkoxide of glycerol is the only Co(II) alkoxide for which a structure has been proposed.[17]

In this paper, we report the synthesis and the structural characterization of monodisperse disk-shaped particles of the cobalt alkoxide of ethanediol. The magnetic properties of this product are presented and discussed relative to its 2D structure and the anisotropic shape of the particles. In the active field of molecule-based magnetic materials, systems of low dimensionality are of particular interest in terms of new magnetic behavior. Systems with high anisotropy are interesting for magnetic information storage, and compounds that combine single-ion and structural anisotropy have been particularly investigated. Single-molecule magnets[18] and single-chain magnets[19] are promising for magnetic storage on the nanometer scale. Here, the slow relaxation of magnetization is responsible for the hysteresis effect at low temperature. There has also been

DOI: 10.1039/b411117f

several studies of 2D systems involving layered compounds showing long-range magnetic ordering and a hysteresis behavior below the critical temperature.[20] Dipolar interactions were proposed to be responsible for a ferromagnetic-like 3D order in these 2D compounds[21] and in some cases very high coercive fields were obtained with a cobalt(II) hydroxide layered phase.[22] The Co(II) compound presented here is a new example of a layered phase with a high uniaxial magnetocrystalline anisotropy.

2. Experimental

2.1 Sample preparation

The cobalt(II) alkoxide was prepared by heating a suspension of cobalt acetate (4 g, 0.016 mol; as the tetrahydrate from Alfa) in ethanediol (200 ml; Acros) to 175 °C. A violet precipitate was first observed when this temperature was reached. This intermediate compound was recovered after 15 min at this temperature and was named CoEGAc. After 30 min at 175 °C the suspension turned progressively pink. The suspension was heated for 2 h and then cooled to room temperature. The pink powder was recovered by centrifugation, washed several times with ethanol and dried in air at 50 °C for one night, and then stored in dry air. In the following, this compound is named CoEG. Under these experimental conditions, no metal was detected by X-ray diffraction. When the water is distilled off completely, another red-pink powder with a different X-ray diffraction pattern appears. This compound will be described elsewhere.

2.2 Characterization

Elemental analysis (Co, C, O, H) was performed at the Service Central d'Analyses (CNRS, Vernaison). Thermal analysis (TGA-TDA) were performed on a Setaram 92-12 apparatus at 20–900 °C under an air flow. Ionic chromatography was performed with a Dionex DX-100 ion chromatograph equipped with AG-4 and AS4-SC columns. Borate buffer solutions were used as the eluent. X-Ray diffraction (XRD) patterns were recorded on a Philips PW1050/25 diffractometer (FeKα_1 and Kα_2 radiations, λ = 1.93597 and 1.93991 Å, respectively). Scanning electron microscopy studies were performed on a Cambridge S-120 microscope. Transmission electron microscopy and electron diffraction studies were performed on a Jeol JEM 2010 UHR operating at 200 kV. The powders were dispersed in ethanol and one drop of the suspension was deposited on the carbon membrane of the microscope grid and the solvent was evaporated at room temperature. The transmission infrared spectra were recorded at 400–4000 cm^{-1} using an Equinox 55 Bruker FT-IR spectrometer. UV-visible spectra were recorded on a Varian Cary 5E spectrophotometer. Magnetic measurements on compacted powders or on films were made on a Quantum Design MPMS-5S SQUID magnetometer at 2–300 K.

3. Results and discussion

3.1 Chemical and thermal analysis

Elemental analysis of compound CoEG (expt. wt %: Co = 48.8; C = 18.9; O = 28.8; H = 3.5%) gave results close to the formula $CoC_2H_4O_2$ (calcd wt %: Co = 49.5; C = 20.2; O = 26.9; H = 3.4%). Ion chromatography revealed the absence of acetate ions. Thermal analysis showed a single weight loss (32.3%) at 250 °C associated with two exothermic peaks, corresponding to the decomposition of the compound. The final product of decomposition at 900 °C was the oxide Co_3O_4, as inferred from X-ray diffraction. The formula weight calculated from this loss, 118.5 g mol^{-1}, is very close to the formula weight: $M(CoC_2H_4O_2)$ = 118.9 g mol^{-1}. An additional weight loss (less than 2%) around 100 °C, corresponding to the departure of water molecules, was observed with some samples. Thus, when cobalt(II) acetate is heated in excess ethanediol, the diol loses its two protons and the dianion complexes the metal center to give a compound with a formula close to the stoichiometry of $Co^{II}(OCH_2CH_2O)$. The cobalt alkoxide of glycerol, $Co^{II}(OCH_2CHOCH_2OH)$, and the nickel alkoxide of ethanediol, $Ni^{II}(OCH_2CH_2O)$, were synthesized under very similar conditions.[15,17] These compounds are very different from the complexes of ethanediol with divalent metal halides, $Co(HOCH_2CH_2OH)_2X_2$, obtained at low temperature and in which the α-diol acts as a ligand.[23]

Elemental analysis of the intermediate compound CoEGAc revealed a much lower cobalt content (≈36%). Thermal analysis revealed a significant weight loss (≈10%) between 70 and 160 °C, corresponding to the departure of water and polyol molecules that are not linked to the cobalt cations. Beyond 250 °C, a weight loss of about 40% is observed, associated with two exothermic peaks corresponding to the decomposition of the compound.

3.2 Infrared spectroscopy

The infrared studies confirmed the absence of acetate ions in the compound CoEG: the ν_{as} and ν_s bands of C=O were not observed. Comparison with the infrared spectrum of ethanediol showed the presence of ethanediolate species in CoEG (Fig. 1). Strong absorptions were observed in the 2850–2950 cm^{-1} range, corresponding to ν_{as} and ν_s C–H bands, and at 1050–1125 cm^{-1}, corresponding to $\rho(CH_2)$, ν(C–O) and ν(C–C) bands.[23] It is noteworthy that the bands in the 1300–1450 cm^{-1} range present in the ethanediol spectrum are no longer observed in the cobalt alkoxide. This can be attributed to the absence of protons in the cobalt alkoxide and thus the disappearance of the δ(C–OH) bands. The CH stretching vibrations in the cobalt alkoxide are split (2954, 2922, 2884 and 2854 cm^{-1}) with respect to ethanediol (2962 and 2877 cm^{-1}). This is the result of a chelating coordination to the cations that lowers the symmetry of the ligand and increases the number of absorptions.[15b] In some samples, an OH stretching vibration was observed as a weak narrow band at 3690 cm^{-1}. This is significantly higher than the value of ν(OH) in cobalt hydroxide (3630 cm^{-1}) and is closer to the ν(OH) of ethanediol in the vapor phase.[23] This absorption corresponds to free OH (*i.e.*, not hydrogen-bonded) belonging to partially deprotonated $C_2H_5O_2^-$ anions. This can be considered as a minor species. A broader band occurring at 3410 cm^{-1} can be attributed to the stretching vibration of OH groups linked by hydrogen bonds. This band is still present after thermal treatment at 200 °C for 5 h under N_2 flow and is most likely the

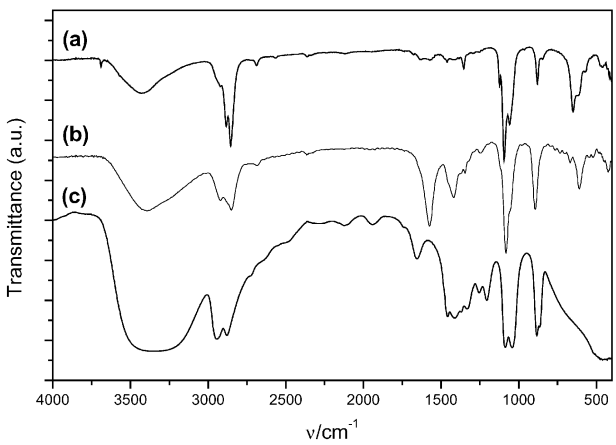

Fig. 1 FTIR spectra of: (a) cobalt alkoxide CoEG; (b) cobalt alkoxyacetate CoEGAc; (c) liquid ethanediol.

result of polyol molecules (partially deprotonated or not) linked to the layers and involved in H bonding.

The IR spectrum of the CoEGAc compound reveals the presence of ethanediolate species with strong absorptions bands in the 2850–2950 cm^{-1} and 1050–1125 cm^{-1} ranges [Fig. 1(b)]. The fact that splitting of the CH stretching vibrations is not observed reveals unidentate coordination mode. The IR spectrum presents also the (C=O) ν_{as} and ν_s bands of acetate ions at 1570 and 1418 cm^{-1}, respectively. These bands are characteristic of unidentate acetates linked to cobalt cations.[13a] Thus, the intermediate compound CoEGAc appears to be a cobalt alkoxyacetate. The broad band corresponding to the OH stretching vibration at 3400 cm^{-1} is much stronger than in the IR spectrum of the CoEG alkoxide. This band is attributed to partially deprotonated diolate species linked by hydrogen bonds and to polyol molecules that are not linked to cobalt cations, as inferred from thermal analysis.

3.3 Morphology

The recovered powders consist in particles in the submicrometer size range and of uniform shape. Scanning electron microscopy studies of the cobalt alkoxide CoEG revealed disk-shaped particles with a diameter varying from 400 nm to 1 μm and a thickness in the 150–300 nm range, depending on samples (Fig. 2). Preferential orientations due to the anisotropic shape of the particles were observed. The two micrographs presented in Fig 2(a,b) are from the same sample but differ in the way the particles were deposited on the microscope support. When the particles were first dispersed in ethanol and a drop of the suspension was deposited on the microscope support, the disk-shaped particles were found to be preferentially oriented sideways [Fig. 2(a)]. When the dry powder was directly deposited on the substrate, the particle orientation was random and lines of edgeways particles could be observed [Fig. 2(b)].

The CoEGAc powder is made up of monodisperse spherical particles with a mean diameter of about 400 nm [Fig. 2(c)]. This different morphology shows that the crystallization of the alkoxide CoEG compound takes place from the solution after re-dissolution of the intermediate alkoxyacetate CoEGAc.

3.4 Structural analysis

3.4.1 X-Ray and electron diffraction. The powder X-ray diffraction pattern of the cobalt alkoxyacetate CoEGAc presents very broad bands characteristic of a very poorly crystallized compound (see inset in Fig. 3). Thus, the 400 nm spheres observed by SEM are polycrystalline with a crystallite size in the nanometer range. A large amount of polyol may be trapped within the porosity of the spheres.

Powder X-ray diffraction and single-area electron diffraction on a single particle showed that the cobalt alkoxide CoEG presents a layered structure derived from the brucite structure with turbostratic disorder along the c axis. The main lines of the X-ray diffraction pattern can be indexed as (00ℓ), (10ℓ) and (11ℓ) in the hexagonal system (Fig. 3). The (00ℓ) lines are narrow, showing a large correlation length along the c axis. The interlayer spacing deduced from the positions of these lines is 8.27 Å. The mean crystallite size, L_{001}, calculated in this direction using the Scherrer formula with the FWHH of the (00ℓ) lines, is 100 nm, that is, close to the particle thickness. Three other lines, at distances of 2.674, 1.547 and 1.340 Å, are strong and are indexed as the (100), (110) and (200) reflections, respectively. Immediately after these lines at larger angles are found the (10ℓ) (11ℓ) and (20ℓ) lines with $\ell \neq 0$, which are much broader. This kind of pattern is characteristic of a turbostratic disorder along the c axis, namely a disorder of positions in the stacking of the (ab) layers. In the brucite structure, the parameter a corresponds to the smallest

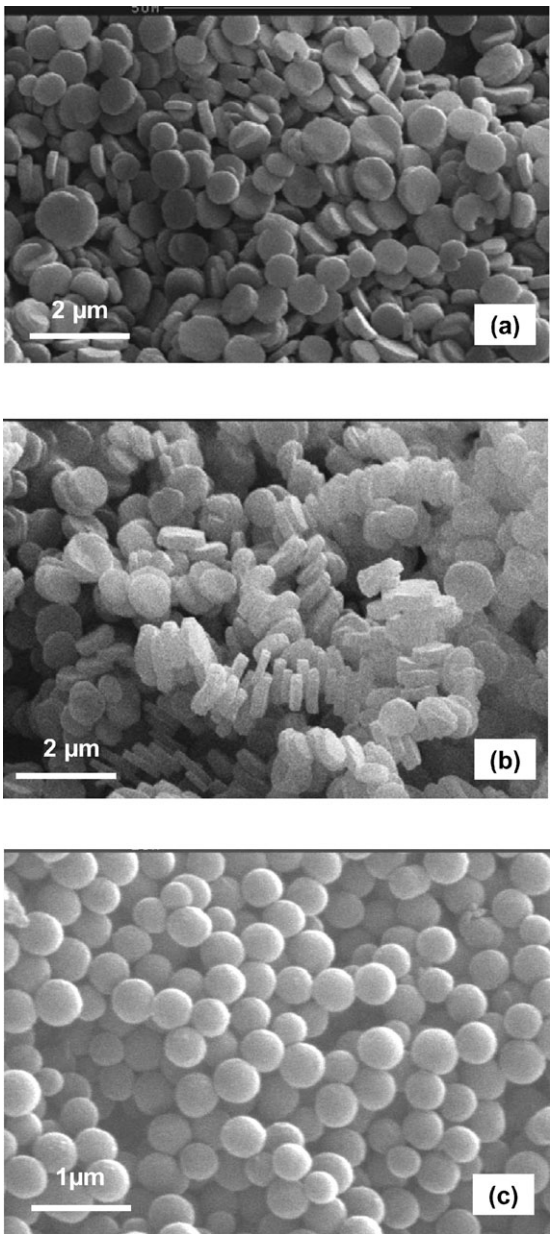

Fig. 2 SEM micrographs of: (a) cobalt alkoxide CoEG (powder dispersed in ethanol and one drop deposited on the aluminium microscope support); (b) cobalt alkoxide CoEG (dry powder directly deposited on the microscope support); (c) intermediate cobalt alkoxyacetate CoEGAc.

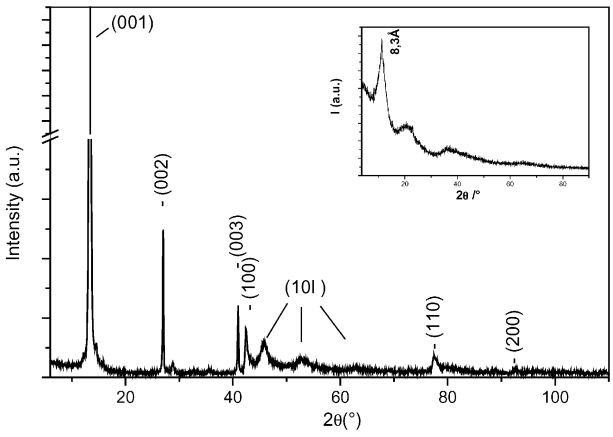

Fig. 3 X-Ray diffraction pattern of cobalt alkoxide CoEG (FeKα radiation). Inset: X-ray diffraction pattern of cobalt alkoxyacetate CoEGAc.

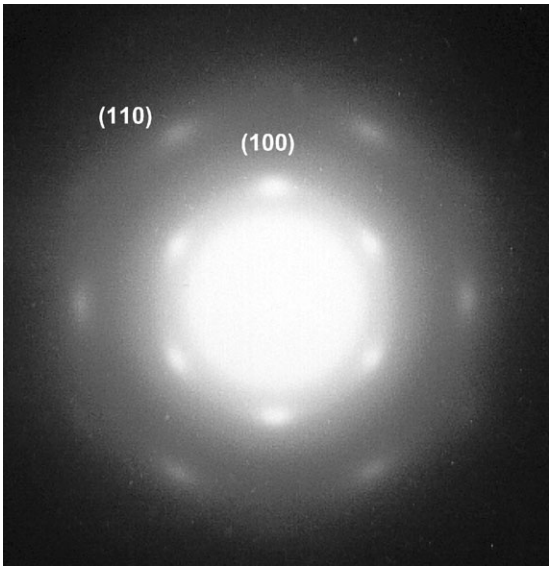

Fig. 4 Selected-area electron diffraction pattern of a single, disk-shaped particle of cobalt alkoxide CoEG with the rotation axis parallel to the electron beam.

metal···metal distance within the triangular array of the (*ab*) layer. In the cobalt alkoxide CoEG this Co···Co distance, deduced roughly from the (100) and (110) positions, is 3.09 Å.

Selected-area electron diffraction was performed on a single platelet with its rotation axis parallel to the electron beam. The pattern can be indexed as the [001] zone axis of the hexagonal structure (Fig. 4). The parameter *a* deduced from this pattern is again 3.09 Å. Furthermore, the diffraction spots are elongated, which reveals the disorder already observed in the X-ray diffraction pattern.

The hydroxides β-$Ni(OH)_2$ and β-$Co(OH)_2$ also crystallize in the brucite structure with an interlayer spacing of 4.62 and 4.65 Å, respectively, and a metal···metal distance within the layer of 3.114 and 3.173 Å, respectively.[24] The nickel alkoxide of ethanediol, $Ni(C_2H_4O_2)$, described by Tekaia-Elhsissen *et al.*,[15b] presents also a structure derived from that of brucite. It crystallizes in the monoclinic system with $a = 5.175$, $b = 6.321$, $c = 8.318$ Å, $\beta = 95.96°$ and with $P2_1/a$ as the likely space group. In this compound the $C_2H_4O_2^{2-}$ dianions chelate the nickel(II) ions. The oxygen atoms of the anions are located at the apices of distorted octahedrons and bridge three metal ions, like the oxygen atom of the hydroxide ions in the brucite structure. The interlayer spacing is occupied by the alkyl chains of the diol. It is 8.318 Å, very close to the distance in the Co(II) compound. Within the layers, the triangular lattice of metal ions presents a monoclinic distortion. The smallest Ni···Ni distances within the layers take values of 3.03 and 3.16 Å, depending on the direction, which is very close to the distance in the Co(II) compound. Thus, by analogy with the nickel compound, the cobalt alkoxide of ethanediol $Co(C_2H_4O_2)$ can be described as a stacking of layers made up of CoO_6 octahedra sharing an edge and with the CH_2CH_2 moieties occupying the interlayer spacing. Distortion within the layers was not seen in this compound. In contrast, turbostratic disorder was observed. Such disorder is frequently observed in solids presenting a layered structure, such as Ni(II) and Co(II) hydroxides.[13,25–27]

Additional, low-intensity lines are observed in the X-ray diffraction pattern (Fig. 3). These lines do not match with a hexagonal cell. They can be attributed to the presence of impurities but were not identified.

3.4.2. UV-visible spectroscopy. The UV-visible absorption spectrum of the cobalt alkoxide CoEG allowed us to confirm

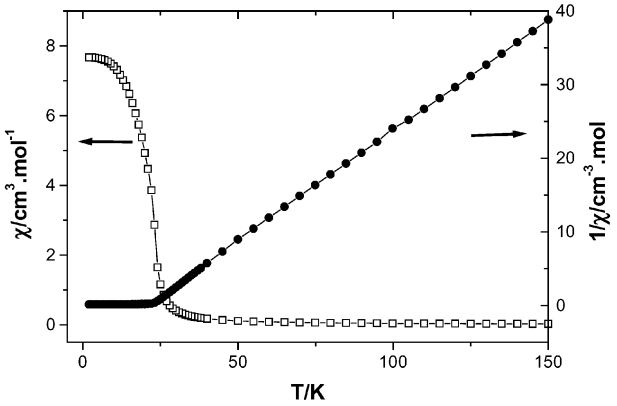

Fig. 5 Temperature dependence of (□) the magnetic susceptibility χ and (●) inverse magnetic susceptibility χ^{-1} of cobalt alkoxide CoEG ($H = 200$ Oe).

that all the cobalt ions are in the +2 valence state and that they occupy an octahedral site with a $^4T_{1g}(F)$ ground state. The absorption at 7940 cm^{-1} (1260 nm) is attributed to the $^4T_{1g}(F) \rightarrow {}^4T_{2g}$ transition, the broad, weak band at 16390 cm^{-1} (610 nm) to the $^4T_{1g}(F) \rightarrow {}^4A_{2g}$ transition and the absorption at 19230 cm^{-1} (520 nm) to the $^4T_{1g}(F) \rightarrow {}^4T_{1g}(P)$ transition.[28] The values of the crystal field strength Dq and the Raccah parameter B, deduced from these energies using the Tanabe–Sugano diagram, are 850 and 790 cm^{-1}, respectively. These values are typical of a CoO_6 octahedron and confirm the conclusions of the diffraction studies. They are very close to those of β-$Co(OH)_2$ ($Dq = 830$ cm^{-1}; $B = 825$ cm^{-1})[29,30] and $Co(HOCH_2CH_2OH)_2Cl_2$ ($Dq = 800$ cm^{-1}; $B = 810$ cm^{-1}).[23] The UV-visible spectrum is very different from those of the hydroxycarboxylates that contain both octahedral and tetrahedral Co(II).[13a,27]

3.5 Magnetic properties

Because of its triangular 2D structure, the magnetic behavior of the cobalt alkoxide CoEG will be described as the result of two kinds of interactions. The first interaction occurs between paramagnetic cation neighbors located within the layers and for which the coordination polyhedra share edges. This leads to strong in-plane interactions *via* a super-exchange mechanism. The second interaction occurs between layers and is much weaker than the in-plane interaction.

The magnetic susceptibility of the cobalt alkoxide CoEG powder was measured at 2–300 K with an applied field H of 200 Oe. The temperature dependence of the susceptibility and the inverse susceptibility $\chi^{-1} = f(T)$ are plotted in Fig. 5 and the temperature dependence of the χT product is plotted in Fig

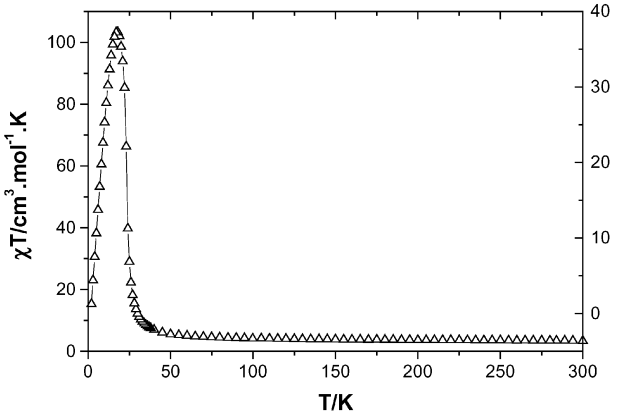

Fig. 6 Temperature dependence of the χT product of cobalt alkoxide CoEG ($H = 200$ Oe).

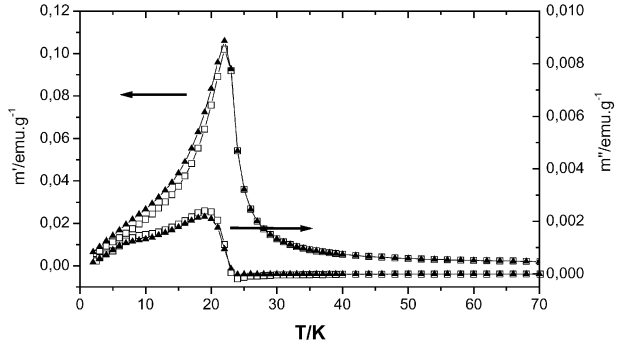

Fig. 7 Temperature dependence of the in-phase (m') and the out-of-phase (m'') components of the ac susceptibility of cobalt alkoxide CoEG powder at (▲) 2 and (□) 500 Hz in zero static field and an oscillating field of 3.5 Oe.

6. At high temperatures, a Curie–Weiss law, $\chi = C/(T-\Theta)$, is observed with $\Theta = +31$ K. This positive value indicates predominant ferromagnetic interactions in the compound. The value of the χT product at 300 K is 3.3 $cm^3\ mol^{-1}$ ($\mu_{eff} = 5.15\ \mu_B$), in good agreement with the molecular formula containing one high-spin Co(II) in an octahedral site. Upon cooling, the χT product increases, as expected for ferromagnetic interactions, and reaches a maximum at 18 K. The susceptibility χ presents a plateau below 20 K that can be related to 3D ferromagnetic order. This is confirmed by ac susceptibility measurements performed at different frequencies. The maxima of the in-phase (m') and the out-of-phase (m'') signals (22 and 19 K, respectively) were independent of the frequency (Fig. 7).

The field dependence of the magnetization measured at 2 K is plotted in Fig. 8. The magnetization presents a hysteresis at low temperature with a remanence and a coercivity H_c of 2500 Oe. At 50 000 Oe the magnetization reaches 2.2 μ_B. This is slightly lower than the saturation magnetization of β-$Co(OH)_2$ (2.87 μ_B) but the alkoxide is not fully saturated at 50 000 Oe. The most striking feature is the remanence-to-saturation ratio (M_r/M_s) of 75%, which is very high for a powder. This gives the hysteresis loop the square aspect usually observed for compounds with uniaxial magnetocrystalline anisotropy and for thin films with perpendicular magnetic anisotropy. Thus, this feature is related to both the anisotropic magnetic properties of the particles and their ability to orient themselves parallel to each other. In order to determine the magnetic easy axis, particles were compacted on a film of capton. As was evidenced by SEM, the particles are oriented sideways, with the c axis perpendicular to the film. The field dependence of the magnetization was measured parallel and perpendicular to the film. Saturation is reached much more easily when the film is perpendicular to the field, despite the demagnetizing effects

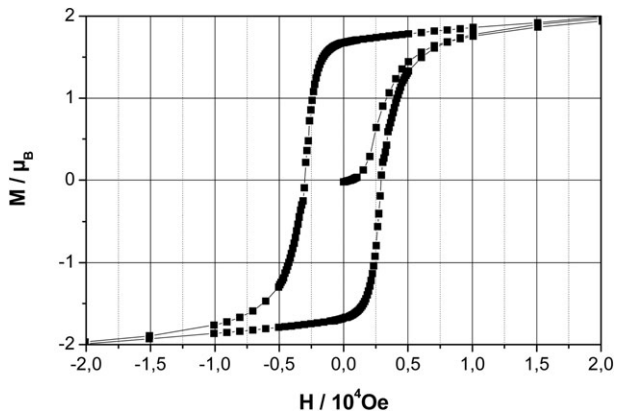

Fig. 8 Field dependence of the magnetization at 2 K of the cobalt alkoxide CoEG powder.

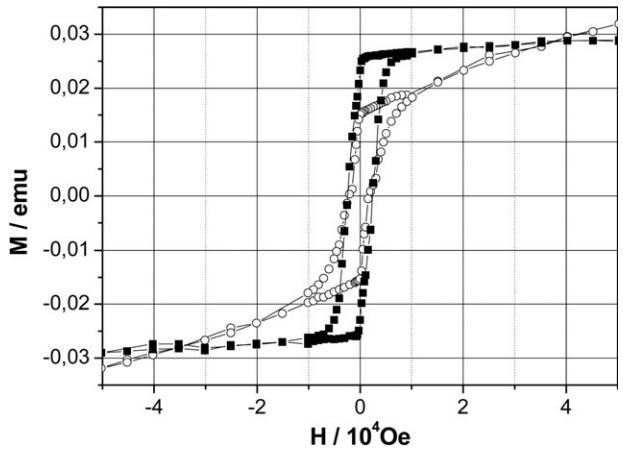

Fig. 9 Field dependence of the magnetization at 2 K of cobalt alkoxide (CoEG) particles, oriented sideways on a film of capton, with the field (■) perpendicular or (○) parallel to the film.

that should align the magnetization in the plane of the film. Conversely, when the film is parallel to the field, saturation is not reached, even at 50 000 Oe (Fig. 9). All these properties point towards a perpendicular anisotropy, that is, an easy axis parallel to the crystallographic c axis.

The magnetic properties of the cobalt alkoxide are summarized in Table 1 and are compared with those of other Co(II) and Ni(II) compounds presenting a brucite-like structure. The antiferromagnetic transition at $T_N = 12.3$ K of β-$Co(OH)_2$ and its metamagnetic behavior are explained by in-plane ferromagnetic interactions and weak interplanar antiferromagnetic interactions.[30,31] The latter are assumed to involve hydrogen bonding within the interlayer spacing. The Co(II) hydroxynitrate presents the same kind of metamagnetic behavior, with a significantly lower critical field corresponding to much weaker interplanar antiferromagnetic interactions.[33] Co(II) hydroxy-*n*-alkylcarboxylates and Co(II) hydroxy-*n*-alkylsulfates, for which the interlayer distance is larger than 10 Å, present spontaneous magnetization due to dipolar interplanar interactions.[32] It must be noted that the hydroxycarboxylate compounds are generally isomorphous to the hydrozincite structure, in which the Co(II) cations are located on both octahedral and tetrahedral sites. This leads to an in-plane ferrimagnetic behavior through predominant antiferromagnetic interactions between the spins of the cations located in the O_h and T_d sites of the same layer. Such a modification of the layers was never observed in the Ni(II) compounds. The in-plane interactions are always ferromagnetic in β-$Ni(OH)_2$,[34] Ni(II) hydroxycarboxylates and Ni(II) hydroxy-*n*-alkylsulfonates.[13b] The magnetic properties of the nickel compounds relative to the basal spacing are similar to those of the cobalt compounds. When the interlayer distance is high enough, the overall magnetic behavior is dominated by the in-plane interactions and 3D ferromagnetic order is observed.[13b,35]

To the best of our knowledge, the cobalt alkoxide $Co(C_2H_4O_2)$ is one of only a very few examples, with β-$Co(OH)_2$ and Co(II) hydroxynitrate, of layered cobalt salts with a pure brucite-like structure, clearly evidenced by UV spectroscopy. In the cobalt alkoxide, all the Co(II) cations occupy an O_h site and the in-plane interaction is ferromagnetic as in β-$Co(OH)_2$. In the latter compound, the super-exchange interaction between the Co(II) spins takes place through the O atoms located at the apices of the CoO_6 octahedra sharing an edge. In the alkoxide, the layer structure is only slightly modified with respect to the hydroxide, and the O atoms belonging to the $(OCH_2CH_2O)^{2-}$ anions can act like the hydroxide groups toward the super-exchange interaction. Moreover, there can be no interplanar exchange pathway in the cobalt alkoxide CoEG because the interlayer spacing is

Table 1 Static magnetic properties of the $Co(C_2H_4O_2)$ alkoxide and of related compounds with similar structures.

	Θ/K	χT^a/cm^3 mol^{-1} K	$\mu_{eff}{}^a/\mu_B$	T_c/K	M^b/μ_B	Ref.
$Co(C_2H_4O_2)$	+31	3.3	5.15	22	2.2	This work
β-$Co(OH)_2$	+20	3.38	5.2	12.3[c]	2.9	31
$Co_2(OH)_3(NO_3)$	—	3.6	5.36	9.8[c]	2.9	32
β-$Ni(OH)_2$	+35	1.28	3.2	30[c]	—	34
$Ni(OH)_{1.5}(Ac)_{0.5}$	+27	1.32	3.25	20	1.9	13b

[a] $T = 300$ K. [b] $H = 50\,000$ Oe. [c] Néel temperature of the antiferromagnetic order.

occupied by the CH_2CH_2 alkyl moieties. Thus, in contrast to the cobalt hydroxide, no metamagnetic behavior was observed but a 3D-like ferromagnetic order. The easy axis is perpendicular to the basal plane, as in β-$Ni(OH)_2$,[34] in Ni(II) hydroxycarboxylates and in Ni(II) hydroxy-*n*-alkylsulfonates.[13b] The smallest distance above which exchange interactions are negligible with respect to dipolar interactions is generally considered to be 10 Å.[21] In the cobalt alkoxide, despite a smaller interlayer spacing, it is very probable that the 3D ferromagnetic order is stabilized by dipolar interactions between layers because of a favorable out-of-plane anisotropy.

4. Conclusion

Disk-shaped particles of a cobalt alkoxide have been prepared by reaction of cobalt acetate in ethanediol near the boiling point. The chemical formula of this compound is very close to the stoichiometric formula $Co(OCH_2CH_2O)$. Structural characterization revealed a brucite-like structure similar to that of the already described nickel alkoxide $Ni(OCH_2CH_2O)$, but with a turbostratic disorder. The magnetic properties show ferromagnetic in-plane interactions, as expected for a layered triangular array of $Co^{II}O_6$ octahedra sharing an edge. The 3D ferromagnetic order is related to a large interplanar distance. Finally, this study shows that control of particle shape and orientation allows one to take advantage of the magnetic anisotropy of a compound.

Acknowledgements

The authors are indebted to F. Warmont (LRS, Paris) for the electron diffraction study, to C. Train (LCIM2, Paris) for access to the SQUID, to V. Cross (UMP Thales-CNRS, Orsay) for fruitful discussions and to Dr J. Lomas (ITODYS, Paris) for his careful reading of the manuscript.

References

1 L. Poul, S. Ammar, N. Jouini, F. Fiévet and F. Villain, *J. Sol-Gel Sci. Technol.*, 2002, **26**, 261.
2 (*a*) F. Bonet, V. Delmas, S. Grugeon, R. Herrera-Urbina, P.-Y. Silvert and K. Tekaia-Elhsissen, *Nanostruct. Mater.*, 1999, **11**, 1277; (*b*) P.-Y. Silvert, R. Herrera-Urbina, N. Duvauchelle, V. Vijayakrishnan and K. T. Elhsissen, *J. Mater. Chem.*, 1996, **6**, 573.
3 N. Chakroune, G. Viau, C. Ricolleau, F. Fiévet-Vincent and F. Fiévet, *J. Mater. Chem.*, 2003, **13**, 312.
4 F. Fiévet, J.-P. Lagier, B. Blin, B. Beaudouin and M. Figlarz, *Solid State Ionics*, 1989, **32/33**, 198.
5 F. Fiévet, F. Fiévet-Vincent, J.-P. Lagier, B. Dumont and M. Figlarz, *J. Mater. Chem.*, 1993, **3**, 627.
6 (*a*) P. Elumalai, H. N. Vasan, M. Verelst, P. Lecante, V. Carles and P. Tailhades, *Mater. Res. Bull.*, 2002, **37**, 353; (*b*) J. K. Vemagiri, S. K. Murthy, R. A. Gunasekaran, P. Coane and K. Varah, *Mater. Lett.*, 2003, **57**, 4098; (*c*) A. Bianco, G. Gusmano, G. Montesperelli, B. Morten, M. Prudenziati, R. Zanoni and G. Righini, *Thin Solid Films*, 2000, **359**, 21; (*d*) C. Luna, M. P. Morales, C. J. Serna and M. Vasquez, *Nanotechnology*, 2004, **15**, S293; (*e*) C. Luna, M. P. Morales, C. J. Serna and M. Vasquez, *Nanotechnology*, 2003, **14**, 268.
7 (*a*) B. Jeyadevan, A. Hobo, K. Urakawa, C. N. Chinnasamy, K. Shinoda and K. Tohji, *J. Appl. Phys.*, 2003, **93**, 7574; (*b*) C. Liu, X. Wu, T. Klemmer, N. Shukla, X. Yang, D. Weller, A. G. Roy, M. Tanase and D. Laughlin, *J. Phys. Chem.*, 2004, **108**, 6121.
8 F. Fiévet, in *Fine Particles: Synthesis, Characterization, and Mechanism of Growth*, ed. T. Sugimoto, Surfactant Science Series, vol. **92**, Marcel Dekker, Inc., New York, 2000, p. 460.
9 (*a*) S. Ammar, A. Helfen, N. Jouini, F. Fiévet, I. Rosenman, F. Villain, P. Molinié and M. Danot, *J. Mater. Chem.*, 2001, **11**, 186; (*b*) S. Chkoundali, S. Ammar-Merah, N. Jouini, F. Fiévet, M. Danot, P. Molinié, F. Villain and J.-M. Grenèche, *J. Phys.: Condens. Matter*, 2004, **16**, 4357; (*c*) J. Merikhi, H. O. Jungk and C. Feldmann, *J. Mater. Chem.*, 2000, **10**, 1311; (*d*) D. Curunti, Y. Remond, N. H. Chou, M. J. Jun, G. Carunti, J. He, G. Goloverda, C. O'Connor and V. Kolesnichenko, *Inorg. Chem.*, 2002, **41**, 6137.
10 (*a*) D. Jézéquel, J. Guenot, N. Jouini and F. Fiévet, *J. Mater. Res.*, 1995, **10**, 77; (*b*) I. R. Collins and S. E. Taylor, *J. Mater. Chem.*, 1992, **2**, 1277.
11 L. Poul, S. Ammar, N. Jouini, F. Fiévet and F. Villain, *Solid State Sci.*, 2001, **3**, 31.
12 R. Bazzi, M. A. Flores, C. Louis, K. Lebbou, W. Zhang, C. Dujardin, S. Roux, B. Mercier, G. Ledoux, E. Bernstein, P. Pierrat and O. Tillement, *J. Colloid Interface Sci.*, 2004, **273**, 191.
13 (*a*) L. Poul, N. Jouini and F. Fiévet, *Chem. Mater.*, 2000, **12**, 3123; (*b*) M. Taibi, S. Ammar, N. Jouini, F. Fiévet, P. Molinié and M. Drillon, *J. Mater. Chem.*, 2002, **12**, 3238.
14 (*a*) N. Jouini, L. Poul, F. Fiévet and F. Robert, *Eur. J. Solid State Inorg. Chem.*, 1995, **32**, 1129; (*b*) L. Poul, N. Jouini, F. Fiévet and P. Herson, *Z. Kristallogr.*, 1998, **213**, 416.
15 (*a*) K. Tekaia-Elhsissen, A. Delahaye-Vidal, G. Nowogrocki and M. Figlarz, *C. R. Acad. Sci., Ser. II: Mec. Phys. Chem. Sci. Terre Univers*, 1989, **309**, 349; (*b*) K. Tekaia-Elhsissen, A. Delahaye-Vidal, G. Nowogrocki and M. Figlarz, *C. R. Acad. Sci., Ser. II: Mec. Phys. Chem. Sci. Terre Univers*, 1989, **309**, 469.
16 D. Larcher, G. Sudant, R. Patrice and J.-M. Tarascon, *Chem. Mater.*, 2003, **15**, 3543.
17 (*a*) P. G. Slade, E. W. Radoslovich and M. Raupach, *Acta Crystallogr., Sect. B*, 1971, **27**, 2432; (*b*) E. W. Radoslovich, M. Raupach, P. G. Slade and R. M. Taylor, *Aust. J. Chem.*, 1970, **23**, 1963.
18 (*a*) T. Mallah and A. Marvilliers, in *Magnetism: Molecules to Materials II*, eds. J. S. Miller and M. Drillon, Wiley–VCH, Weinheim, 2001, p. 189; (*b*) V. Marvaud, C. Decroix, A. Scuiller, C. Guyard-Duhayon, J. Vaissermann, F. Gonnet and M. Verdaguer, *Chem.-Eur. J.*, 2003, **9**, 1677.
19 (*a*) A. Caneschi, D. Gatteschi, N. Lalioti, C. Sangregorio, R. Sessoli, G. Venturi, A. Vindigni, A. Rettori, M. G. Pini and M. A. Novak, *Eur. Phys. Lett.*, 2002, **58**, 771; (*b*) R. Lescouëzec, J. Vaissermann, C. Ruiz-Pérez, F. Lloret, R. Carrasco, M. Julve, M. Verdaguer, Y. Dromzee, D. Gatteschi and W. Wersdorfer, *Angew. Chem., Int. Ed.*, 2003, **42**, 1483.
20 P. Rabu, M. Drillon, K. Awaga, W. Fujita and T. Sekine, in *Magnetism: Molecules to Materials II*, eds. J. S. Miller and M. Drillon, Wiley–VCH, Weinheim, 2001, p. 357.
21 M. Drillon and P. Pannisod, *J. Magn. Magn. Mater.*, 1998, **188**, 93.
22 (*a*) Z.-L. Huang, M. Drillon, N. Masciocchi, A. Sironi, J.-T. Zhao, P. Rabu and P. Panissod, *Chem. Mater.*, 2000, **12**, 2805; (*b*) M. Kurmoo, *Chem. Mater.*, 1999, **11**, 3370.
23 D. Knetsch and W. L. Groeneveld, *Inorg. Chim. Acta*, 1973, **7**, 81.
24 JCPDS files n° 74-2075 for β-$Ni(OH)_2$ and n° 74-1057 for β-$Co(OH)_2$.

25 C. Tessier, P. H. Haumesser, P. Bernard and C. Delmas, *J. Electrochem. Soc.*, 1999, **146**, 2059.
26 S. LeBihan and M. Figlarz, *J. Cryst. Growth*, 1972, **13/14**, 458.
27 M. Kurmoo, *J. Mater. Chem.*, 1999, **9**, 2595.
28 A. B. P. Lever, *Inorganic Electronic Spectroscopy*, Elsevier, Amsterdam, 2nd edn., 1984.
29 A. Ludi and W. Feitknecht, *Helv. Chim. Acta*, 1963, **46**, 2226.
30 M. Andrut and M. Wildner, *J. Phys.: Condens. Matter*, 2001, **13**, 7353.
31 T. Takada, Y. Bando, M. Kiyama, H. Miyamoto and T. Sato, *J. Phys. Soc. Jpn.*, 1966, **21**, 2726.
32 P. Rabu, S. Angelov, P. Legoll, M. Belaiche and M. Drillon, *Inorg. Chem.*, 1993, **32**, 2463.
33 V. Laget, C. Hornick, P. Rabu, M. Drillon and R. Ziessel, *Coord. Chem. Rev.*, 1998, **178–180**, 1533.
34 T. Takada, Y. Bando, M. Kiyama, H. Miyamoto and T. Sato, *J. Phys. Soc. Jpn.*, 1966, **21**, 2745.
35 M. Kurmoo, P. Day, A. Derory, C. Estournès, R. Poinsot, M. J. Steat and C. J. Kepert, *J. Solid State Chem.*, 1999, **145**, 452.